JOURNAL OF COMPUTATIONAL PHYSICS 79, 477–483 (1988)

Note

Contour Dynamics/Surgery on the Sphere

1. Introduction

This note derives remarkably simple equations governing the motion of an inviscid fluid of constant but negligible depth on the surface of a sphere and outlines an associated numerical algorithm. The algorithm offers an alternative approach for investigating idealised geophysical flows.

Inviscid, incompressible flow on a spherical surface and on an infinite plane share the property that the vorticity normal to the surface is conserved on fluid particles. Material conservation of vorticity implies that one may consider the simple piecewise-constant subclass of vorticity distributions for which the boundaries of vorticity discontinuity or *contours* alone determine the dynamics of the flow; in the planar case [1], the velocity at a point $\mathbf{x}$ is given by

$$\frac{d\mathbf{x}}{dt} = -\frac{1}{4\pi}\sum_k \tilde{\omega}_k \oint_{C_k} \log|\mathbf{x}-\mathbf{x}_k|^2\, d\mathbf{x}_k \tag{1}$$

where $\mathbf{x}_k$ is a point on the kth contour C_k across which the vorticity jumps by $\tilde{\omega}_k$ crossing the contour inwards. The inside of C_k is to the left of $d\mathbf{x}_k$. Equation (1) is true for all points $\mathbf{x}$ in the fluid, but when $\mathbf{x}$ lies on one of the contours, (1) forms a closed system for the evolution of the contours in terms of their instantaneous positions. Zabusky *et al.* [6] coined the term "contour dynamics" for this system. Perhaps surprisingly, it turns out (see below) that the *same* equation, appropriately interpreted, also governs inviscid flow on the sphere.

Consider then the generalisation of (1) to the spherical case. Juckes [4] and more recently Kimura and Okamoto [5] have derived contour dynamical equations in terms of spherical coordinates, and Juckes has performed several short-time calculations with hemispheric symmetry. The first step is to invert Laplace's equation $\nabla^2\psi = \omega$ to get the streamfunction $\psi(\theta, \phi)$ (θ being colatitude and ϕ longitude) in terms of the vorticity distribution $\omega(\theta, \phi)$, and this involves finding the Green's function $G(\theta, \phi; \theta', \phi')$ for the spherical Laplacian operator. It is a simple matter to show that

$$G = \frac{1}{4\pi}\log(1-\cos\Theta) \tag{2}$$

where $\cos\Theta = \cos\theta\cos\theta' + \sin\theta\sin\theta'\cos(\phi-\phi')$ is simply the dot product of the

0021-9991/88 $3.00

two position vectors $\mathbf{x} = (\sin\theta\cos\phi, \sin\theta\sin\phi, \cos\theta)$ and $\mathbf{x}' = (\sin\theta'\cos\phi', \sin\theta'\sin\phi', \cos\theta')$ on the unit sphere. The streamfunction is therefore given by

$$\psi(\theta,\phi) = \frac{1}{4\pi}\iint \omega(\theta',\phi')\log(1-\cos\Theta)\,d\Omega' \tag{3}$$

where $d\Omega' = \sin\theta'\,d\theta'\,d\phi'$ is just the incremental area.

The contour dynamical equations are obtained from (3) by assuming that the vorticity distribution is piecewise constant. Without loss of generality, consider a single vorticity interface across which the vorticity jumps by $\tilde{\omega}$. The components of the velocity are given in terms of derivatives of the streamfunction as

$$\begin{aligned} \frac{d\theta}{dt} &= u_\theta = -\frac{1}{\sin\theta}\frac{\partial\psi}{\partial\phi}, \\ \sin\theta\frac{d\phi}{dt} &= u_\phi = \frac{\partial\psi}{\partial\theta}. \end{aligned} \tag{4}$$

Thus, from the first of these equations and (3),

$$\begin{aligned} \sin\theta\frac{d\theta}{dt} &= -\frac{\tilde{\omega}}{4\pi}\iint \frac{\partial}{\partial\phi}\log(1-\cos\Theta)\sin\theta'\,d\theta'\,d\phi' \\ &= +\frac{\tilde{\omega}}{4\pi}\iint \frac{\partial}{\partial\phi'}\log(1-\cos\Theta)\sin\theta'\,d\theta'\,d\phi' \\ &= -\frac{\tilde{\omega}}{4\pi}\oint_C \log(1-\cos\Theta)\sin\theta'\,d\theta'. \end{aligned} \tag{5}$$

The second line follows from the symmetry of G in its arguments ϕ and ϕ', and the third line follows from Stokes' theorem. In the final expression, θ' and ϕ' are to be regarded as tracing out the contour C.

A much simpler set of equations results if one works with Cartesian coordinates constrained to the unit sphere. With $z = \cos\theta$, (5) can be rewritten as

$$\frac{dz}{dt} = -\frac{\tilde{\omega}}{4\pi}\int_C \log(1-\cos\Theta)\,dz'. \tag{6}$$

Furthermore, notice that $\cos\Theta = \mathbf{x}\cdot\mathbf{x}'$ and $1-\cos\Theta = \frac{1}{2}|\mathbf{x}-\mathbf{x}'|^2$—$G$ is symmetric in $\mathbf{x}$ and $\mathbf{x}'$. It is this property of G that implies (6) is equally true for the other two coordinates x and y (z, z' are replaced by x, x' and y, y'). Hence, (1) describes motion on the plane when $\mathbf{x}$ is a two-dimensional vector and motion on the sphere when $\mathbf{x}$ is a three-dimensional vector. Apart from the dimensionality of $\mathbf{x}$, *indentical equations describe fluid motion on the plane and on the sphere.*

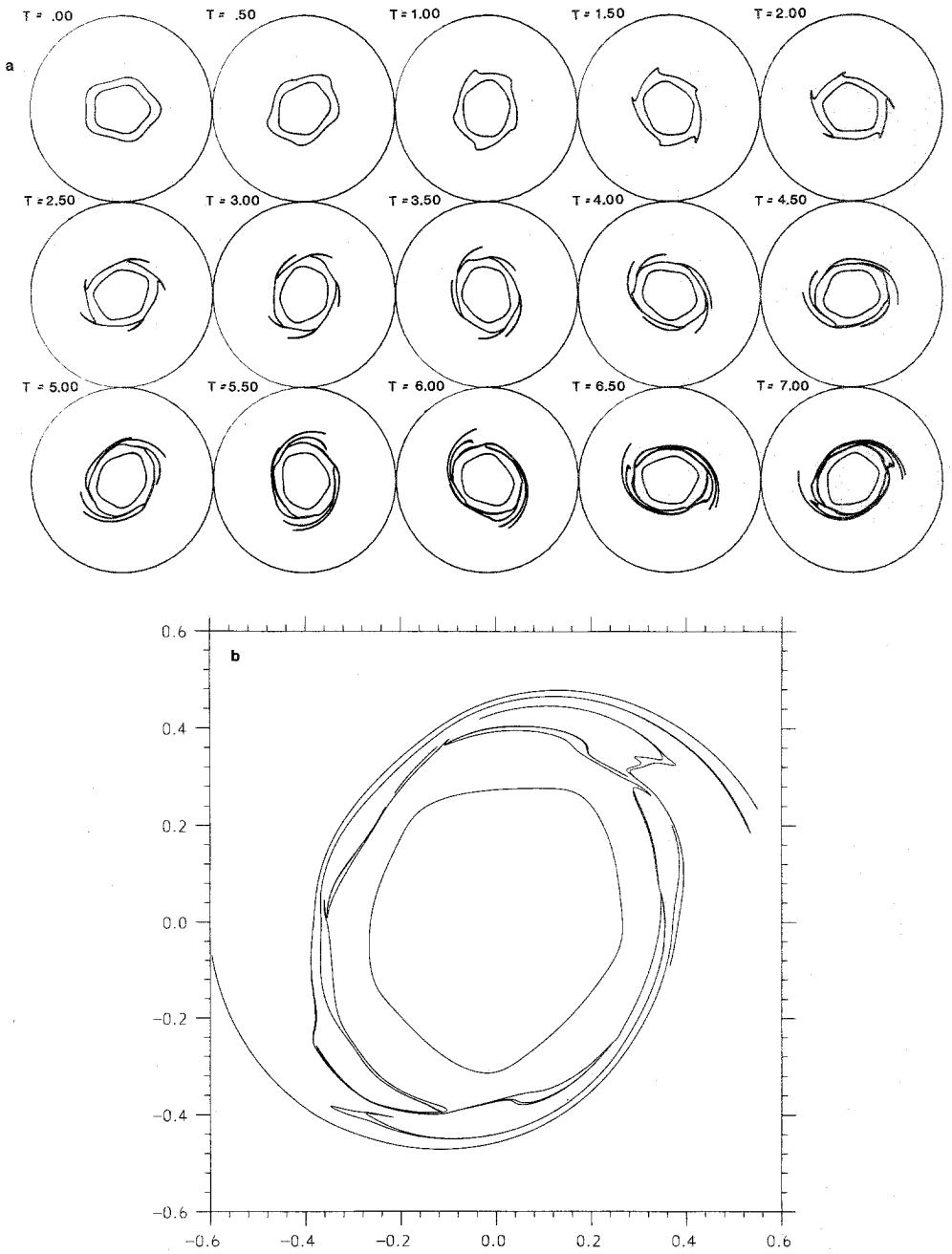

FIG. 1. (a) A polar stereographic projection of vortex flow on the sphere (plotted is $\hat{x} = x/(1+z)$ $\hat{y} = y/(1+z)$ for the northern hemisphere ($z \geq 0$) only. Time increases across and downwards. Algorithm parameters (see [2]): $\Delta t = 0.05$, $\mu = 0.04$, and $\delta = 10^{-4}$. (b) An enlarged view of the flow at $t = 7.25$.

2. An Example Calculation

A single example is presented to demonstrate the feasibility and simplicity of performing spherical calculations. The "countour surgery" algorithm [2] devloped for planar flow was converted to the spherical case. Both algorithms feature surgery or the automatic removal of fine-scale vorticity features, adaptive node adjustment for the nodes or points whose union make up a given contour, nonlinear interpolation of the curve between successive nodes, and an explicit calculation of the contour integral between each pair of nodes that is accurate to first order in the departure of the contour from a line segment between nodes. The only significant difference between the two algorithms arises from the curvature of the spherical surface: on the sphere, the curve between two nodes must follow the spherical surface and is necessarily curved. This and other minor differences are outlined in the Appendix.

The example calculation begins with two nested contours centred on the north pole ($z=1$). The vorticity jumps by π across each contour going inwards (toward the north pole). Initially, $x=0.7a\cos\alpha$, $y=0.6a\sin\alpha$, and $z=\sqrt{(1-x^2-y^2)}$, $0\leqslant\alpha\leqslant 2\pi$ (with $a=0.7938$ and 1 for the inner and outer contours, respectively), modified by the fivefold perturbation $0.05a\cos 5\alpha$ (see Figs. 1a and b). The waves on the outer contour proceed to steepen and break and continue breaking over the duration of the calculation, and long, thin filaments wrap around the vortex. This process of "filamentation" also occurs in planar geometry; for details and comparisons between planar and spherical geometry, see [3].

3. Conclusions

It is now possible to efficiently perform numerical calculations of inviscid, incompressible, flow on the sphere for piecewise-constant vorticity distributions. The emphasis of present research lies on the differences between planar and spherical flow, in such problems as the form of equilibria, the stability of equilibria, vortex merger, and the "filamantation" of vorticity interfaces.

Appendix

The contour surgery algorithm outlined in a previous paper [2] is virtually unchanged when applied to flow on a sphere. Below, the unobvious differences between the planar and spherical algorithm are discussed.

Interpolation

Each contour is approximated by a finite number of nodes and an associated set of interpolation coefficients. Between two nodes, say $\mathbf{x}_i$ and $\mathbf{x}_{i+1}$, the contour is assumed to take the form (see Fig. 2)

$$\mathbf{x}(p)=\mathbf{x}_i+p\mathbf{t}_i+\eta(p)\mathbf{n}_i+\xi(p)\bar{\mathbf{x}}_i \tag{A1}$$

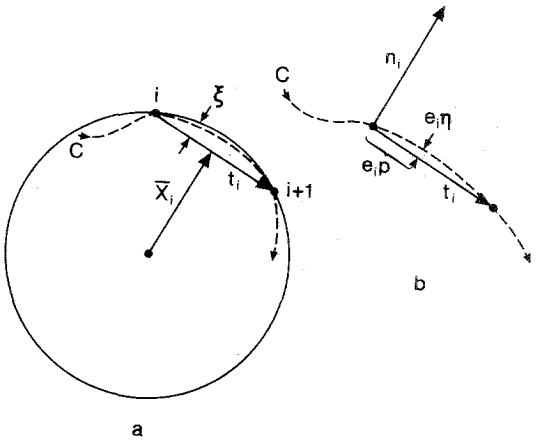

FIG. 2. The interpolation between two nodes, i and $i+1$, along a contour C (dashed line) lying on the surface of a sphere. (a) An on-edge view looking in the direction of $\mathbf{n}_i$. The variation of C in the direction of $\bar{\mathbf{x}}_i$ is a parabolic arc ξ to leading order in the distance e_i between the two nodes. (b) A view looking down on $\bar{\mathbf{x}}_i$. The variation of C in the direction of $\mathbf{n}_i$ is assumed to be a cubic polynomial $e_i\eta$ whose variation is weak compared with e_i.

where $\mathbf{t}_i = \mathbf{x}_{i+1} - \mathbf{x}_i$, $\mathbf{n}_i = \mathbf{x}_i \times \mathbf{x}_{i+1}$, and $\bar{\mathbf{x}}_i = \frac{1}{2}(\mathbf{x}_i + \mathbf{x}_{i+1})$ are mutually orthogonal vectors; $\eta(p) = \alpha_i p + \beta_i p^2 + \gamma_i p^3$, $0 \leqslant p \leqslant 1$, describes the nonlinear variation of the contour in a plane perpendicular to $\bar{\mathbf{x}}_i$; and $\xi(p) = \frac{1}{2}e_i^2\, p(1-p)$, $e_i = |\mathbf{t}_i| = |\mathbf{n}_i|$, is the new term arising from the curvature of the spherical surface itself, terms of $O(e_i^4)$ being neglected. It is assumed that nodes are sufficiently close together that $\eta \ll 1$ and $\xi \ll e_i$.

The coefficients α_i, β_i, and γ_i are calculated in terms of the curvature κ_i at $\mathbf{x}_i$ in a plane perpendicular to $\mathbf{x}_i$ and the curvature at $\mathbf{x}_{i+1}$, κ_{i+1}—these formulae may be found in [2]. For clarity, the expression for the curvature used is

$$\kappa_i = \frac{2\mathbf{x}_i \cdot (\mathbf{x}_+ \times \mathbf{x}_-)}{|\mathbf{x}_+ e_-^2 - \mathbf{x}_- e_+^2|} \tag{A2}$$

where $\mathbf{x}_\pm = \mathbf{x}_{i\pm1} - \mathbf{x}$.

Node Redistribution

At each time step, all of the nodes are redistributed so as to put more nodes in regions of high curvature and fewer in regions of low curvature. This distribution actually depends on a nonlocal function of curvature which is sensitive not only to curvature but also to its rate of change. In the spherical algorithm, the total curvature $\sqrt{(1+\kappa_i^2)}$—the root mean square of the spherical curvature (unity) and the curvature orthogonal to the spherical surface—is used. Finally, in the planar case, it is necessary to define a length typical of the large scales, L; for the unit sphere, L is set to 1.

Velocity Field Determination

The velocity field contributed by the segment between two nodes is explicitly evaluated to first order in the small departure of the contour from the cord separating the nodes. In the planar case, it was shown that this correction leads to a significant increase in the order of accuracy of the algorithm [2]. Similar benefits can be expected in the spherical case.

The algorithm for calculating the velocity at a point $\mathbf{x}$ is virtually identical to the planar algorithm, aside from the dimensionality of the vectors. The differences are pointed out following the outline of the velocity algorithm, which follows next:

$$\frac{d\mathbf{x}}{dt}=\frac{1}{2\pi}\sum_k \tilde{\omega}_k \sum_i T_i\mathbf{t}_i+N_i\mathbf{n}_i+S_i\bar{\mathbf{x}}_i \tag{A3}$$

where, supressing unessential subscripts, the following quantities are all evaluated at node i:

$$\begin{aligned}
T&=1-BL-(1-B)\,L_+-G^2I_0+C[\alpha I_1+\beta I_2+\gamma I_3]+D[I_1-I_2],\\
N&=\alpha J_1+\beta J_2+\gamma J_3,\\
S&=\tfrac{1}{2}e^2[J_1-J_2],\\
A&=|\mathbf{x}-\mathbf{x}_i|^2/e^2,\\
B&=\mathbf{t}\cdot(\mathbf{x}-\mathbf{x}_i)/e^2,\\
C&=\mathbf{n}\cdot(\mathbf{x}-\mathbf{x}_i)/e^2,\\
D&=\tfrac{1}{2}\bar{\mathbf{x}}\cdot(\mathbf{x}-\mathbf{x}_i),\\
G&=|\mathbf{t}\times(\mathbf{x}-\mathbf{x}_i)|/e^2,\\
L&=\log|\mathbf{x}-\mathbf{x}_i|,\\
L_+&=\log|\mathbf{x}-\mathbf{x}_{i+1}|,\\
I_0&=\frac{1}{G}\left(\tan^{-1}\frac{B}{G}+\tan^{-1}\frac{1-B}{G}\right),\\
I_1&=L_+-L+BI_0,\\
I_n&=\frac{1}{n-1}+2BI_{n-1}-AI_{n-2},\qquad n\geqslant 2,\\
J_n&=I_{n+1}-BI_n,\qquad n\geqslant 1.
\end{aligned} \tag{A4}$$

If the evaluation point happens to be close to the segment connecting $\mathbf{x}_i$ and $\mathbf{x}_{i+1}$, close in the sense that $A-B<0$, then the procedure above is slightly modified: with $h=\eta(B)$, h is subtracted from C, $2Ch-h^2$ is subtracted from A with the consequent changes to G, etc., and ChI_0 is subtracted from T.

This algorithm is identical to the planar case if G is used in place of C and terms involving D and $\bar{\mathbf{x}}_i$ are dropped.

Surgery

No significant differences arise other than the use of three-dimensional vectors in place of two-dimensional ones.

Errors due to imperfect interpolation, imperfect evaluation of the velocity field, a finite time step, and surgery result in slightly displacing nodes off the sphere. When this occurs, points are adjusted in the direction of $\mathbf{x}_i$ so that $|\mathbf{x}_i| = 1$.

ACKNOWLEDGMENT

I thank Martin Juckes for bringing this problem to my attention.

REFERENCES

1. G. S. DEEM AND N. J. ZABUSKY, *Phys. Rev. Lett.* **40**, 859 (1978). Also in: *Solitons in Action* (Academic, New York, 1978), p. 277.
2. D. G. DRITSCHEL, *J. Comput. Phys.* **77**, 240 (1988).
3. D. G. DRITSCHEL, *J. Fluid Mech.* **194**, 511 (1988).
4. M. N. JUCKES, Rayleigh Essay Prize, University of Cambridge, England, 1986 (unpublished).
5. Y. KIMURA AND H. OKAMOTO, private communication (1987).
6. N. J. ZABUSKY, M. H. HUGHES, AND K. V. ROBERTS, *J. Comput. Phys.* **30**, 96 (1979).

RECEIVED: July 8, 1987; REVISED: January 13, 1988

DAVID G. DRITSCHEL

Department of Applied Mathematics
and Theoretical Physics
University of Cambridge
Silver Street
Cambridge CB3 9EW, England